



Differential intrinsic functional connectivity changes in semantic variant primary progressive aphasia



Giovanni Battistella^{a,*}, Maya Henry^b, Benno Gesierich^a, Stephen M. Wilson^c,
Valentina Borghesani^a, Wendy Shwe^a, Zachary Miller^{a,d}, Jessica DeLeon^a, Bruce L. Miller^a,
Jorge Jovicich^e, Nico Papinutto^f, Nina F. Dronkers^{g,h}, William W. Seeley^a,
Maria Luisa Mandelli^{a,d}, Maria Luisa Gorno-Tempini^{a,d}

^a Memory and Aging Center, Department of Neurology, University of California, San Francisco, CA 94158, USA

^b Department of Communication Sciences and Disorders, University of Texas, Austin, USA

^c Department of Hearing and Speech Sciences, Vanderbilt University Medical Center, Nashville, TN 37232, USA

^d Department of Neurology, Dyslexia Center, University of California, San Francisco, CA 94158, USA

^e Center for Mind/Brain Sciences (CIMEC), University of Trento, Rovereto, Italy

^f Department of Neurology, University of California, San Francisco, CA 94158, USA

^g Department of Psychology, University of California, Berkeley, CA 94720, USA

^h Department of Neurology, University of California, Davis, CA 95616, USA

ARTICLE INFO

Keywords:

Primary progressive aphasia
Functional connectivity
Resting-state connectivity
Language
Parietal lobe

ABSTRACT

The semantic variant of primary progressive aphasia (svPPA) is a clinical syndrome characterized by semantic memory deficits with relatively preserved motor speech, syntax, and phonology. There is consistent evidence linking focal neurodegeneration of the anterior temporal lobes (ATL) to the semantic deficits observed in svPPA. Less is known about large-scale functional connectivity changes in this syndrome, particularly regarding the interplay between affected and spared language networks that leads to the unique cognitive dissociations typical of svPPA.

Using whole-brain, seed-based connectivity on task-free Magnetic Resonance Imaging (MRI) data, we studied connectivity of networks anchored to three left-hemisphere regions crucially involved in svPPA symptomatology: ATL just posterior to the main atrophic area, opercular inferior frontal gyrus, and posterior inferior temporal lobe. First, in 32 healthy controls, these seeds isolated three networks: a ventral semantic network involving anterior middle temporal and angular gyri, a dorsal articulatory-phonological system involving inferior frontal and supramarginal regions, and a third functional connection between posterior inferior temporal and intraparietal regions likely involved in linking visual and linguistic processes. We then compared connectivity strength of these three networks between 16 svPPA patients and the 32 controls. In svPPA, decreased functional connectivity in the ventral semantic network correlated with weak semantic skills, while connectivity of the network seeded from the posterior inferior temporal lobe, though not significantly different between the two groups, correlated with pseudoword reading skills. Increased connectivity between the inferior frontal gyrus and the superior portion of the angular gyrus suggested possible adaptive changes.

Our findings have two main implications. First, they support a functional subdivision of the left IPL based on its connectivity to specific language-related regions. Second, the unique neuroanatomical and linguistic profile observed in svPPA provides a compelling model for the functional interplay of these networks, being either up- or down-regulated in response to disease.

1. Introduction

Primary progressive aphasia (PPA) is a clinical syndrome characterized by progressive speech and language deficits caused by

selective neurodegeneration of specific brain networks (Mesulam, 2001; Gorno-Tempini et al., 2004). In the semantic variant PPA (svPPA, or semantic dementia), damage to the anterior temporal lobe (ATL) is associated with impaired semantic memory, manifesting with

* Corresponding author at: UCSF Memory and Aging Center, Mission Hall Building, 505 16th street, Room 5131, San Francisco, CA 94158, USA.

E-mail address: Giovanni.Battistella@ucsf.edu (G. Battistella).

<https://doi.org/10.1016/j.nicl.2019.101797>

Received 1 February 2019; Accepted 26 March 2019

Available online 27 March 2019

2213-1582/ © 2019 The Authors. Published by Elsevier Inc. This is an open access article under the CC BY-NC-ND license

(<http://creativecommons.org/licenses/by-nc-nd/4.0/>).

difficulties in confrontation naming, object recognition, word comprehension and reading of words with irregular letter-sound correspondence (e.g., Hodges et al., 1992; Binney et al., 2016). In the early phases of the disease, motor speech, syntax, and phonological processing and their corresponding brain networks are instead relatively preserved in svPPA.

Decades of neuroimaging research using lesion-to-symptoms mapping or Positron Emission Tomography (PET) have identified the role of the ATL in determining semantic deficits in svPPA and in other disorders affecting this region (e.g., Mummery et al., 1999; Patterson et al., 2007b; Schwartz et al., 2009; Mion et al., 2010). On the other hand, few functional imaging studies with task-based PET and fMRI have been performed in svPPA (e.g., Mummery et al., 1999; Sonty et al., 2003; Wilson et al., 2009), mainly because of the difficulty in applying such technique in patients who cannot perform the cognitive task of interest (Price et al., 2006). The introduction of task-free fMRI (Raichle, 2006) overcame this problem, allowing the investigation of functional dynamics in focal neurodegenerative diseases (Guo et al., 2013; Mandelli et al., 2016; Collins et al., 2017) with selective vulnerability for specific brain networks (Seeley et al., 2009). These studies provided new evidence that degeneration in a crucial network node can cause large-scale altered activation pattern within and between networks (Pievani et al., 2014; Tahmasian et al., 2016).

Two studies that have applied task-free fMRI to svPPA showed reduced ATL connectivity with primary and modality-selective association cortices (Guo et al., 2013; Agosta et al., 2014). However, the svPPA syndrome also is characterized by a marked dissociation between impaired semantic processing and spared motor speech and phonological functions, and as a result, patients rely on phonological strategies to compensate for their deficits. An example of such strategies is the regularization errors that patients with svPPA make while attempting to read irregular words using their spared orthographic-to-phonological reading strategy (reading the word “yacht” as “yach-dt” or “island” as “is-land”). Such a strategy typically is applied only in reading pseudo-words, but in svPPA patients, who have lost knowledge of irregular spellings, it is the only available reading mechanism (Wilson et al., 2009; Binney et al., 2016). Studying the functional dynamics associated with both impaired and spared language functions in svPPA would provide evidence for the functional interplay of large-scale language networks in determining this unique linguistic and clinical profile.

In this study, we combined seed-based task-free-fMRI (tf-fMRI) connectivity and neuropsychological data in a cohort of svPPA patients and healthy controls (HC) to investigate activations in the intrinsic brain networks anchored to key regions associated with spared and impaired language functions in svPPA (motor speech and phonology vs. semantics). By selecting our seeds based on previous fMRI findings, we predicted that the resulting networks would reiterate functionally-distinct language processing networks. We also hypothesized that partially-distinct patterns of functional connectivity would be found between HC and svPPA patients, indicating potential markers for clinical phenotype and disease severity.

2. Materials and methods

2.1. Participants

All subjects were right-handed and gave written informed consent for their participation in the study. The experimental procedures were approved by the Committees on Human Research at the University of California, San Francisco (UCSF). We studied two groups of participants. The first group of 32 healthy participants (14 males / 18 females; mean age: 64 ± 5.1 years) was used to define language-related functional connectivity networks and statistically compare their connectivity with the patient group. Sixteen patients with svPPA (9 males / 7 females; mean age: 62.2 ± 5.9 years) were used to probe the pattern of language-related functional connectivity networks in a

Table 1
Demographic, clinical, and neuropsychological characteristics of patients and controls.

| Variables | svPPA | Controls |
|---|-------------|---------------|
| Demographics | | |
| Age | 62.5 ± 5.9 | 64.0 ± 5.1 |
| Sex (M/F) | 9/7 | 14/18 |
| Education (years) | 17.0 ± 2.6 | 17.6 ± 2.0 |
| Clinical | | |
| Mini Mental Status Examination (30) | 26.5 ± 2.2 | 29.4 ± 0.8 * |
| Clinical Dementia Rating | 0.7 ± 0.4 | 0 ± 0 * |
| Clinical Dementia Rating (sum of boxes) | 4.1 ± 2.9 | 0.0 ± 0.1 * |
| Age at disease onset | 55.9 ± 7.3 | N/A ± N/A |
| Years from first symptoms | 6.0 ± 3.8 | N/A ± N/A |
| Language production | | |
| Confrontation naming (BNT, 15) | 6.4 ± 4.0 | 14.5 ± 0.6 * |
| Phonemic fluency (D words in 1 min) | 7.3 ± 3.1 | 15.0 ± 4.0 * |
| Semantic fluency (Animals in 1 min) | 8.7 ± 3.3 | 24.1 ± 4.1 * |
| Speech fluency (WAB, 10) | 8.9 ± 0.7 | 10.0 ± 0.0 |
| Apraxia of speech rating (MSE, 7) | 0.0 ± 0.0 | 0.0 ± 0.0 |
| Dysarthria rating (MSE, 7) | 0.0 ± 0.0 | 0.0 ± 0.0 |
| Repetition (WAB, 100) | 92.8 ± 7.0 | 99.5 ± 0.9 |
| Language comprehension | | |
| Auditory word recognition (PPVT, 16) | 10.0 ± 4.2 | 15.9 ± 0.4 * |
| Sequential commands (WAB, 80) | 76.5 ± 7.2 | 80.0 ± 0.0 |
| Semantic knowledge (PPT–P, 52) | 42.4 ± 7.2 | 51.8 ± 0.4 |
| Reading | | |
| Regular words (100) | 96.8 ± 6.0 | 100.0 ± 0.0 |
| Exception words (100) | 87.0 ± 16.3 | 99.8 ± 0.6 |
| Pseudo-words (100) | 90.7 ± 12.2 | 97.8 ± 3.6 |
| Spelling | | |
| Regular words (40) | 18.9 ± 2.2 | N/A ± N/A |
| Exception words (40) | 16.1 ± 4.7 | N/A ± N/A |
| Pseudo-words (20) | 19 ± 2.6 | N/A ± N/A |
| Visuospatial function | | |
| Modified Rey–Osterrieth copy (17) | 15.5 ± 1.0 | 15.0 ± 1.1 |
| Visual memory | | |
| Modified Rey–Osterrieth delay (17) | 6.2 ± 4.8 | 12.5 ± 2.0 * |
| Verbal memory | | |
| CVLT-MS trials 1–4 (40) | 19.3 ± 6.4 | 28.7 ± 3.1 |
| CVLT-MS 30 s free recall (10) | 3.9 ± 2.5 | 7.9 ± 1.6 |
| CVLT-MS 10 min free recall (10) | 2.3 ± 2.4 | 7.3 ± 1.6 |
| Executive function | | |
| Digit span backwards | 4.8 ± 0.8 | 5.7 ± 1.1 * |
| Modified trails (lines per minute) | 21.0 ± 10.0 | 37.7 ± 10.2 * |
| Calculation (5) | 4.6 ± 0.5 | 4.8 ± 0.4 |

Values are means ± SD. * Significantly impaired relative to controls, $p < .05$.

Since the present control group was not tested on these variables, we used data from Gorno-Tempini et al. (2004) and an independent group of 17 healthy participants to test differences in these scores between a control population and the svPPA patients enrolled in this study. BNT, Boston Naming Test; WAB, Western Aphasia Battery; MSE, Motor Speech Evaluation; PPVT, Peabody Picture Vocabulary Test; PPT–P, Pyramids and Palm Trees-Pictures; CVLT-MS, California Verbal Learning Test-Mental Status. See Kramer et al. (2003) for a detailed description of neuropsychological testing procedures and Gorno-Tempini et al. (2004) for a detailed description of language testing procedures.

neurodegenerative population. All participants were recruited at the Memory and Aging Center (MAC) at the University of California, San Francisco (UCSF, USA) and received comprehensive multidisciplinary evaluations including neurological history and examination, neuropsychological testing, and neuroimaging, as previously described (Gorno-Tempini et al., 2004). A multidisciplinary team diagnosed patients with probable svPPA according to consensus clinical criteria (Gorno-Tempini et al., 2011). Demographic, clinical, and

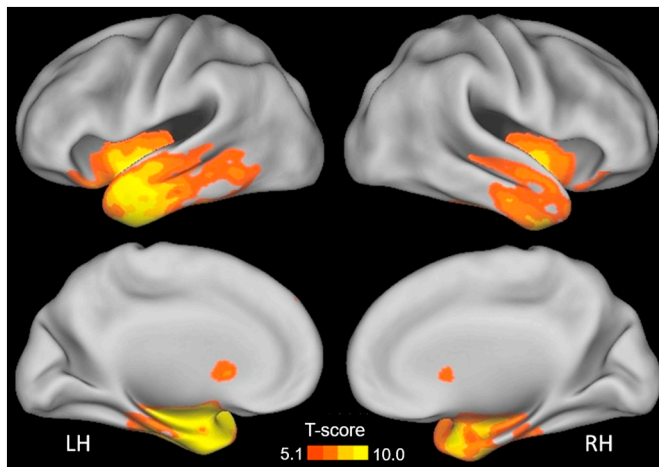


Fig. 1. Atrophy pattern in svPPA patients. The map was thresholded at p (FWE) $< .05$ using a permutation approach, and is shown on a rendered surface of the Montreal Neurological Institute (MNI) template. Colorbar represents T-score.

neuropsychological characteristics for patients and healthy age-matched controls are provided in Table 1. To better characterize the patient group in relation to previous studies, we examined global atrophy patterns in svPPA patients using voxel-based morphometry (VBM). Details about the methods are described in the dedicated section below. We observed the expected pattern of atrophy, involving the bilateral medial and lateral temporal lobes, as well as the bilateral insula (see Fig. 1). The neuropsychological evaluations show the typical clinical profile (Table 1).

2.2. Neuroimaging protocol

The neuroimaging protocol for all participants included a high-resolution structural scan for inter-subject registration and atrophy assessment of svPPA patients, as well as an echo-planar imaging (EPI) scan to study task-free functional connectivity. Participants were instructed to remain still and keep their eyes closed without falling asleep during the acquisition of tf-fMRI data.

Participants were scanned with a Siemens 3 Tesla Trio scanner using a body transmit coil and an 8-channel receive head coil. A T1-weighted 3D Magnetization Prepared Rapid Acquisition Gradient Echo (MPRAGE) was acquired with 160 sagittal slices, echo time (TE)/repetition time (TR)/inversion time (TI) = 2.98/2300/900 ms, flip angle = 9° , $1 \times 1 \times 1$ mm resolution, field of view = 256×256 mm, matrix = 256×256 . For tf-fMRI, 240 T2*-weighted volumes were acquired with an EPI protocol consisting of 36 AC/PC-aligned axial slices acquired in interleaved order. The following acquisition parameters were utilized: TR/TE = 2000/27 ms, flip angle = 80° , slice thickness = 3 mm with 0.6 mm gap, field of view = 230×230 mm, matrix = 92×92 .

2.3. Voxel-based morphometry (VBM)

Structural MRI data were pre-processed and analyzed using Statistical Parametric Mapping (SPM8, Wellcome Department of Cognitive Neurology, London, UK, <http://www.fil.ion.ucl.ac.uk/spm/software/spm8>). For VBM analysis, T1-weighted data were classified as grey matter (GM), white matter (WM), and cerebrospinal fluid (CSF) using the unified segmentation approach (Ashburner and Friston, 2005). GM probability maps were normalized to the Montreal Neurological Institute (MNI) space, modulated by the Jacobian determinant of the deformations derived from the spatial normalization, and smoothed with an isotropic Gaussian kernel of 8 mm full width at half

maximum (FWHM). Voxel-based inferential statistic was performed by fitting a general linear model entering age, gender, and total intracranial volume (TIV) as covariates. The statistical map showing GM volume differences between HC and svPPA was thresholded at $p < .05$, corrected for multiple comparisons using a permutation approach (Wilson et al., 2010). Statistical maps were calculated for 1000 random permutations of subjects' group-identities, and the largest T statistic in each map was used to determine the null distribution of maximum T statistic.

2.4. Tf-fMRI data preprocessing

The analysis of functional data was performed using SPM8 and MATLAB (MathWorks, Natick, MA). The first 5 volumes of the acquisition were discarded to allow T₁ equilibrium to be established. Preprocessing and seed-based functional connectivity analyses were performed following an optimized procedure (Weissenbacher et al., 2009). Functional images first were corrected for slice timing and checked for excessive motion after the realignment of the volumes to the mean functional image. None of the participants exceeded a maximum of 2 mm for relative head motion, a maximum of 2° for relative rotation, and a maximum of 10% of the total frames with motion spikes, calculated as relative motion > 1 mm. The mean functional image then was co-registered with the MPRAGE using a rigid body transformation. Tf-fMRI data were normalized to the MNI space using the parameters calculated from the normalization of the MPRAGE, and spatially smoothed with a Gaussian kernel of 5 mm FWHM. Functional data were corrected further for noise using a multiple linear regression against the 6 rigid body realignment parameters, resulting from the head motion correction, the average white matter signals received from 4 cubic ROIs in the bilateral frontal and parietal WM, the ventricular system signal, and the global signal. The residual data were band-pass filtered (0.0083–0.15 Hz).

2.5. Seed-based functional connectivity analysis

Single-subject correlation maps were generated by calculating the correlation coefficient between the average Blood-Oxygen Level Dependent (BOLD) signal time-course from the seed ROIs (described in the next section) and the time-course from all other voxels of the brain. Correlation maps were converted to z-scores by Fisher's r-to-z transformation to enable parametric statistical comparisons. Within-subject group analysis for each of the three groups and language networks was performed using a one-sample *t*-test. The resulting group level connectivity maps were thresholded at $p < .05$, corrected for whole-brain family-wise error (FWE) using Gaussian Random Field theory implemented in SPM8. To account for the smaller number of svPPA patients compared to the number of age-matched controls, the group-level maps for the svPPA patients were thresholded voxel-wise at $p < .001$. We used a different threshold only for the visualization of the results, and for the qualitative description of the regions included in each of the three networks.

2.6. Functional definition of intrinsic language networks – seed ROI definition

Language-related intrinsic functional connectivity networks were identified in healthy controls by calculating group-level connectivity maps for the three language-relevant seeds. These three seed-ROIs were defined as $9 \times 9 \times 9$ mm boxes, derived by combining evidence from neuroimaging and cognitive studies in PPA, neuropsychological studies on other patients' populations, and task-based fMRI studies in healthy controls. The overall goal was to identify networks related to spared or impaired functions in svPPA (see Fig. 2).

The first seed, included for its relevance in articulatory and phonological processes that are relatively spared in svPPA, was centered in

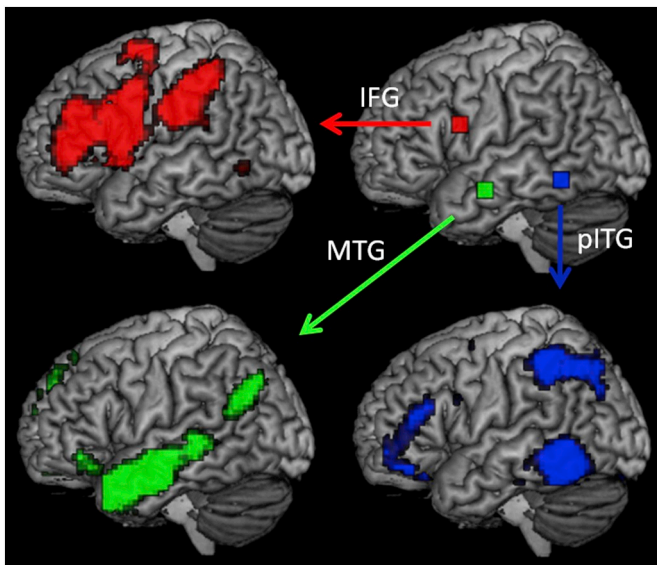


Fig. 2. Functional connectivity networks in healthy controls ($p < .05$, FWE corrected; height threshold $T = 5.88$). Right upper panel shows the location of the three seeds in the left opIFG (red), left aMTG (green), and the left pITG (blue). Arrows point to the network revealed by each of these seeds. Left hemispheres are shown.

the left posterior, opercular part of the IFG (opIFG) and in particular at the activation peak (MNI coordinates $x = -50$, $y = 8$, $z = 23$). This specific coordinate was identified in a previous study by contrasting a phonemic fluency task against semantic and syntactic fluency ones (Heim et al., 2008). The 9-mm box centered on these coordinates (also considering the smoothing kernel) includes regions that are: atrophic in the nonfluent/agrammatic variant of PPA (nfvPPA; (Gorno-Tempini et al., 2004; Grossman, 2012; Mandelli et al., 2016)); identified as the frequently lesioned epicenter in post-stroke Broca's aphasia cases (Hillis et al., 2004); and associated with articulatory/phonological processes by numerous fMRI activation studies (Brunswick et al., 1999; Bonilha et al., 2006; MacSweeney et al., 2009), as evidenced by a meta-analysis conducted in the Neurosynth toolbox (Yarkoni et al., 2011). We hypothesized that this seed would be functionally connected with the supramarginal portion of the IPL, as evidenced by previous findings (Mandelli et al., 2016). We also hypothesized that this network would be functionally normal in svPPA in relation to spared motor speech and phonological processing.

The second seed was located in the ATL, a region known to be involved in semantic processing. We did not position the seed within the temporal pole, epicenter of the disease in svPPA, because of extreme atrophy in these patients that could confound our results. Instead, we chose a seed in the left anterior middle temporal gyrus (aMTG) as previously and successfully implemented in a study of task-free fMRI in svPPA (Guo et al., 2013). The 9-mm box seed was centered at the activation peak (MNI coordinates $x = -60$, $y = -6$, $z = -18$) and was identified by contrasting a semantic association task on pairs of famous faces against a perceptual matching task related to pairs of unknown faces (Gesierich et al., 2012). This aMTG 9-mm box included regions that are: consistently atrophic in svPPA (Gorno-Tempini et al., 2004; Patterson et al., 2007b); linked to semantic deficits in patients with stroke and herpes encephalitis (Noppeney et al., 2007); and activated by semantic tasks in healthy subjects (Vandenberghe et al., 1996; Gorno-Tempini et al., 2000; Mechelli et al., 2007; Binder et al., 2009b; Simmons et al., 2010), as evidenced by meta-analysis conducted in the Neurosynth toolbox. We hypothesized that the network anchored in the aMTG would be functionally connected to the angular portion of the IPL as evidenced by previous findings (Jackson et al., 2016). We also hypothesized that this network would show decreased connectivity in

svPPA as compared to controls, in relation to their semantic deficits. In particular, we hypothesized that other non-atrophic areas connected with the ATL also would show patterns of decreased connectivity.

The third seed was defined in the left posterior ITG (pITG), a key language region that is located posterior to the ATL pattern of atrophy seen in svPPA and that has been previously implicated in compensatory processes in a PET activation study in svPPA patients performing a semantic judgment task (Mummery et al., 1999). This region is considered as an important gateway hub involved in linking visual association areas with phonological and linguistic processes in superior temporal and IPL areas (Price, 2000, 2012). The center of this 9-mm seed box was placed at the peak activation of the above-mentioned study (MNI coordinates $x = -54$, $y = -52$, $z = -10$). The pITG 9-mm box centered on these coordinates included regions that are: involved in the logopenic variant of PPA that is characterized by phonological deficits and phonological dyslexia (Gorno-Tempini et al., 2008); lesioned in stroke patients with picture naming deficits (Foundas and Vasterling, 1998; Baldo et al., 2013); and activated consistently by reading, naming and repetition tasks in activation studies of healthy subjects (Price and Friston, 1997; Cohen et al., 2004; Fairhall and Caramazza, 2013). This multimodal language region also is adjacent to the so-called visual word form area (Stevens et al., 2017) and has been identified to be involved in orthographic, semantic and phonological processing in the Neurosynth toolbox. We hypothesized that this network should be connected to the superior angular/intraparietal sulcus region (Wilson et al., 2009; Purcell et al., 2011; Vogel et al., 2012) and might be involved in partially-spared pseudoword reading (exception word reading associated with middle temporal atrophy). Thus, we hypothesized that there would be no differences in functional connectivity between svPPA and controls in this network.

2.7. Functional connectivity changes in the language networks between svPPA and HC

To determine quantitative functional connectivity changes in svPPA patients, we compared single-subject connectivity maps in patients and controls for each of the three language networks. Given the spatial distribution of the identified networks in healthy controls (see Result section), these group comparisons were masked to include only voxels located in the IPL: the supramarginal gyrus (SMG), the intraparietal sulcus (IPS) and the angular gyrus (AG), as defined by the Pickatlas tool (Maldjian et al., 2003) and using the anatomical parcellation of the MNI brain created by Tzourio-Mazoyer and colleagues (Tzourio-Mazoyer et al., 2002). We used a single ROI covering the whole IPL instead of the anatomical networks defined in healthy controls in order to utilize a larger anatomical mask not restricted only to specific portions of the IPL found in controls. Resulting statistical maps were thresholded first voxelwise at $p < .01$, and then at the cluster level at $p < .05$ (FWE small volume corrected for the IPL mask).

To assess whether observed group differences could be explained by underlying grey matter atrophy in either the seed ROI or in the single voxels for which connectivity was estimated, we re-estimated the models, entering the voxel-wise grey matter probability maps and the average grey matter probability in the seed ROI as covariates using the Biological Parametric Mapping toolbox (Casanova et al., 2007). Grey matter probability maps were derived during the segmentation of the structural images in SPM8 (described above) and were smoothed to the same degree as the functional images (Gaussian kernel of 5 mm FWHM).

2.8. Correlation of functional connectivity with cognitive scores

In svPPA patients, we performed correlation analyses between the z-scores of functional connectivity extracted from the IPL sub-regions showing maximum connectivity to each of the seeds and relevant behavioral measures associated with the proposed functional role of the

language networks. We selected an auditory word recognition test (an abbreviated version of the Peabody Picture Vocabulary Test, PPVT, Kramer et al., 2003) as a surrogate test of semantic processing. Pseudoword reading (from the Arizona Reading List, Beeson, 2010), due to its reliance on subword-level analysis of letter strings and their mapping onto plausible phonemes, was selected to test for orthography-to-phonology conversion. As svPPA patients' performance on phonological and motor speech tasks (as detected with selected sub-test of the Western Aphasia Battery, Kertesz, 1982) was at ceiling, we did not test the correlation between connectivity and these behavioral measures. Similarly, we could not perform the same correlation analyses in healthy controls because all behavioral measures were at ceiling in this group. As a control measure, we also included a visuo-spatial processing score that we hypothesized would not associate with any of the functional networks (modified version of Benson figure copy, Kramer et al., 2003). Relationships between the behavioral variables and the extracted z-scores were determined using Spearman partial correlations removing the effect of disease severity in each correlation by controlling for the Clinical Dementia Rating (CDR) score.

3. Results

3.1. Definition of language networks in controls and svPPA

In healthy controls (HC), the network resulting from the left opIFG seed included areas in the bilateral opercular and triangular part of the IFG, left middle frontal gyrus, bilateral SMG and IPS, left putamen, left anterior cingulate cortex, and left ITG (Fig. 2, Table 2). The network resulting from the left aMTG seed included areas in bilateral MTG, temporal pole, ITG, precuneus, hippocampus, and parahippocampal gyrus. Additional significant regions were located in the left AG, anterior insula, orbital IFG, anterior and posterior cingulate cortices, as well as in the right middle occipital, and orbital medial frontal gyrus (Fig. 2, Table 2). The use of a dedicated sequence optimized to reduce signal drop-out in the temporal lobes in an additional group of healthy controls confirmed the spatial distribution of this network (Supplementary file 1). The network resulting from the left pITG seed included areas in the bilateral ITG, left IPS, bilateral triangular IFG, and left precentral gyrus (Fig. 2, Table 2).

Interestingly, all three networks included peak locations in different portions of the IPL, thereby functionally segmenting the region into distinct areas. The aMTG-seeded network was connected to the inferior portion of the AG (Brodmann area BA 39), while the main IPL targets of the opIFG- and pITG- seeded networks were the SMG (BA40, anterior portion) and IPS (BA 40/7), respectively. The networks originated by seeding in the aMTG and opIFG slightly overlapped in the anterior IPS, whereas the aMTG seed did not show any overlap with the remaining networks.

SvPPA patients showed the involvement of similar regions to controls in the three networks (Fig. 3, panel C).

3.2. Comparison of IPL functional connectivity between HC and svPPA patients

Compared to age-matched controls, svPPA patients showed stronger connectivity between opIFG and the dorsal-posterior portion of the superior AG (maximum $T = 3.97$; MNI coordinates: $x = -39$, $y = -64$, $z = 55$; cluster extent 4644 mm^3 ; $p = .001$, FWE corrected, Fig. 4, panel A). While this cluster did not overlap with the dorsal network in controls, it did overlap partially with the dorsal network in svPPA (volume of overlap, 459 mm^3). Inversely, patients showed decreased connectivity between the aMTG seed and the inferior part of the AG (maximum $T = 3.93$; MNI coordinates: $x = -48$, $y = -67$, $z = 34$; cluster extent 1350 mm^3 ; $p = .048$, FWE corrected) (Fig. 4, panel B). This cluster overlapped with the inferior portion of the AG connected to the aMTG via the ventral network in controls and svPPA. There was no

significant difference in connectivity between controls and patients in the network connecting the pITG to the IPS. The increased connectivity in the IFG network was independent of grey matter atrophy (maximum $T = 4.02$; MNI coordinates $-48 -64 43$; cluster $p = .002$, FWE corrected), while the effect of decreased functional connectivity in the aMTG network was no longer significant when including grey matter volumes in the seed as a covariate.

3.3. Correlations of behavioral measures with functional connectivity

In svPPA patients, we found significant correlations between aMTG-to-AG connectivity and PPVT scores ($r = 0.6$, $p = .03$), and between pITG-to-IPS connectivity and the percentage of correctly read pseudo-words ($r = 0.64$, $p = .01$). All other correlations were not significant (Fig. 5).

4. Discussion

The present study applied whole-brain, seed-based connectivity to task-free fMRI data in healthy controls to identify three functionally and anatomically segregated left hemisphere networks involved in spared and impaired language processes in svPPA. We found that these networks were connected to discrete areas within the IPL: a dorsal system involving inferior frontal and supramarginal regions; a relatively more ventral network involving anterior middle temporal and angular gyri; and a third network linking posterior inferior temporal and intraparietal regions. These results suggest unique roles for distinct sub-regions of the IPL in phonological-articulatory vs. semantic functions. Also, we propose that the third more posterior network, connecting the posterior inferior temporal cortex to a region in the intraparietal sulcus, may mediate processes related to sub-lexical orthography-to-phonology conversion. This is supported further by the correlation between functional connectivity within this network and the percentage of correctly read pseudo-words in svPPA, suggesting an alternate mechanism for processing written language in the face of damage to semantic representations.

Individuals with svPPA showed spared intrinsic functional connectivity in the orthography-to-phonology conversion network, decreased connectivity in the ventral semantic network, and increased connectivity in the dorsal articulatory-phonological network (observed between the inferior frontal gyrus and the superior portion of the angular gyrus), consistent with their language profiles. The up-regulation of the dorsal network suggests a dynamic reorganization of the dorsal pathway in response to degeneration of the anterior temporal lobes.

4.1. The role of the inferior parietal lobule in language

The involvement of the inferior parietal lobule (IPL) in language processing is well-established (Humphreys and Lambon Ralph, 2015; Jung et al., 2018), with references dating back to classic neurological models (Gerstmann, 1957). Far from being a unitary construct, the IPL is a collection of important anatomical, cytoarchitectonic, and functional subdivisions (Nelson et al., 2010; Achal et al., 2016; Wang et al., 2016). Standard parcellations distinguish the angular and supramarginal gyri, but cytoarchitectonic and anatomical atlases define boundaries within and between these two structures with a high degree of variability (Caspers et al., 2006). Previous MR-based functional and structural connectivity studies in healthy controls (HC) have parcellated the IPL (Podzebenko et al., 2005; Nelson et al., 2010; Garcea and Mahon, 2014; Ruschel et al., 2014; Achal et al., 2016; Wang et al., 2016; Wang et al., 2017). Our study determined the degree to which heterogeneous IPL sub-regions might contribute to specific language processes in healthy controls and svPPA patients. The following sections of the Discussion will detail the specific involvement of each of the portions of the IPL in relation to the language functions attributed to each of the intrinsic networks.

Table 2
Functional connectivity maps for the three language-related seeds in HC.

| Seed | Brain area | MNI coordinates | | | Extent (mm ³) | P (FWE) | Max T | |
|-------------------------------------|---|-------------------------------|-----|-----|---------------------------|---------|---------|-------|
| | | x | y | z | | | | |
| opIFG | Left inferior frontal opercular | -51 | 9 | 21 | 14,256 | < 0.001 | 31.1 | |
| | <i>Left inferior frontal triangular</i> | -42 | 36 | 15 | | | 9.23 | |
| | <i>Left middle frontal orbital</i> | -42 | 48 | -9 | | | 7.91 | |
| | Right inferior frontal opercular | 51 | 9 | 24 | 6291 | < 0.001 | 12.85 | |
| | Left inferior parietal | -54 | -30 | 45 | 13,824 | < 0.001 | 12.64 | |
| | <i>Left supramarginal</i> | -60 | -27 | 36 | | | 11.35 | |
| | <i>Left intraparietal</i> | -45 | -45 | 54 | | | 8.18 | |
| | Left putamen | -27 | 15 | 3 | 5724 | < 0.001 | 10.59 | |
| | <i>Left pallidum</i> | -21 | 0 | 3 | | | 9.36 | |
| | Right supramarginal | 60 | -15 | 27 | 6183 | < 0.001 | 10.29 | |
| | <i>Right supramarginal</i> | 51 | -33 | 42 | | | 8.71 | |
| | Right inferior frontal triangular | 48 | 39 | 6 | 2268 | < 0.001 | 10.21 | |
| | Left superior parietal | -21 | -60 | 51 | 351 | < 0.001 | 8.72 | |
| | Right insula | 39 | 0 | 3 | 648 | < 0.001 | 8.16 | |
| | Left anterior cingulum | 3 | 3 | 27 | 324 | 0.003 | 7.7 | |
| | Left inferior temporal | -54 | -57 | -6 | 459 | 0.004 | 7.53 | |
| | aMTG | Left middle temporal | -60 | -9 | -18 | 26,001 | < 0.001 | 29.1 |
| | | <i>Left anterior insula</i> | -30 | 3 | -12 | | | 13.58 |
| | | <i>Left inferior temporal</i> | -39 | 6 | -33 | | | 12.74 |
| Right middle temporal | | 60 | 0 | -21 | 13,554 | < 0.001 | 15.79 | |
| <i>Right superior temporal pole</i> | | 39 | 15 | -30 | | | 12.43 | |
| <i>Right middle temporal pole</i> | | 48 | 12 | -24 | | | 11.99 | |
| Right middle occipital | | 48 | -63 | 24 | 3591 | < 0.001 | 14.45 | |
| Left precuneus | | -6 | -54 | 36 | 17,334 | < 0.001 | 12.65 | |
| <i>Right precuneus</i> | | 0 | -63 | 21 | | | 12.41 | |
| <i>Left precuneus</i> | | -6 | -51 | 9 | | | 11.07 | |
| Left angular | | -45 | -66 | 27 | 6912 | < 0.001 | 12.31 | |
| Right parahippocampal | | 24 | -15 | -21 | 3105 | < 0.001 | 11.83 | |
| Left inferior frontal orbital | | -45 | 30 | -9 | 702 | < 0.001 | 10.84 | |
| Right medial frontal orbital | | 6 | 54 | -9 | 5265 | < 0.001 | 9.74 | |
| <i>Right rectus</i> | | 6 | 33 | -18 | | | 8.06 | |
| <i>Left anterior cingulum</i> | | -6 | 45 | 6 | | | 7.51 | |
| pITG | | Left inferior temporal | -54 | -51 | -15 | 9531 | < 0.001 | 33.08 |
| | | <i>Left inferior temporal</i> | -60 | -36 | -21 | | | 10.29 |
| | | Left intraparietal | -33 | -51 | 36 | 6426 | < 0.001 | 11.5 |
| | <i>Left intraparietal</i> | -42 | -48 | 45 | 11.43 | | | |
| | Right inferior temporal | 63 | -51 | -12 | 1863 | < 0.001 | 10.27 | |
| | Right inferior frontal triangular | 51 | 36 | 15 | 324 | < 0.001 | 8.65 | |
| | Left precentral | -48 | 12 | 33 | 567 | < 0.001 | 8.34 | |
| | Left inferior frontal triangular | -42 | 36 | 15 | 864 | < 0.001 | 8.28 | |

Note: P values (P) and maximum T statistics (Max T) are reported for the peak voxel of each cluster. P values were controlled for FWE. For single clusters, which cover larger cortical areas or extend into different areas of the brain, the local maxima in these additional areas are indicated in italics.

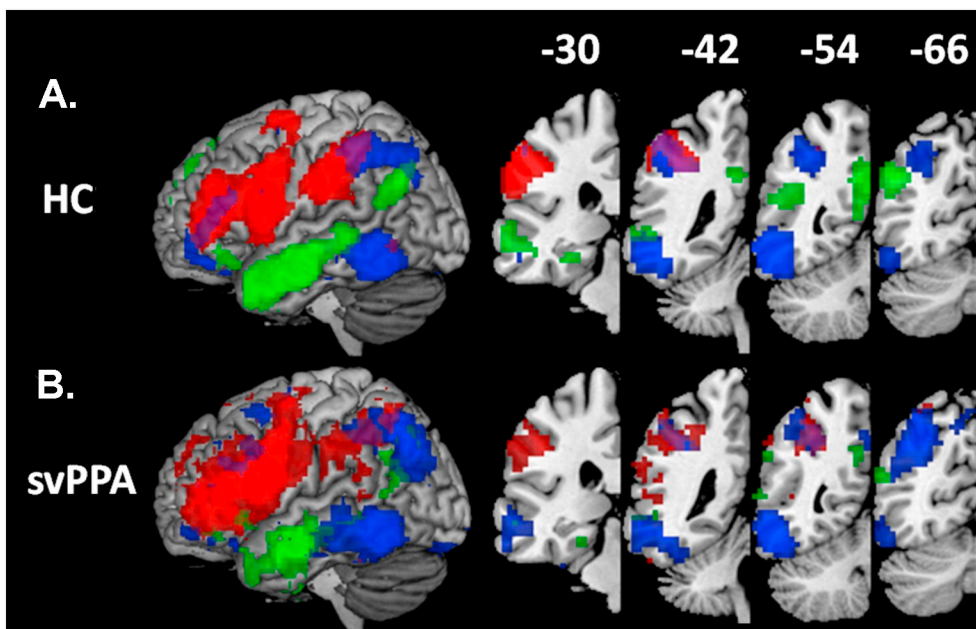


Fig. 3. The three language networks in the two subject groups. Networks are colored according to the colors of the seeds shown in Fig. 2: opIFG network (red); aMTG network (green); pITG network (blue). Maps in HC, (panel A) are thresholded at $p < .05$, FWE corrected (height threshold $T = 5.88$), and voxel-wise at $p < .001$ for the svPPA patients (height threshold $T = 3.73$, panel B) to account for the smaller number of svPPA patients. A surface rendering, as well as coronal IPL sections, is shown for the left hemisphere.

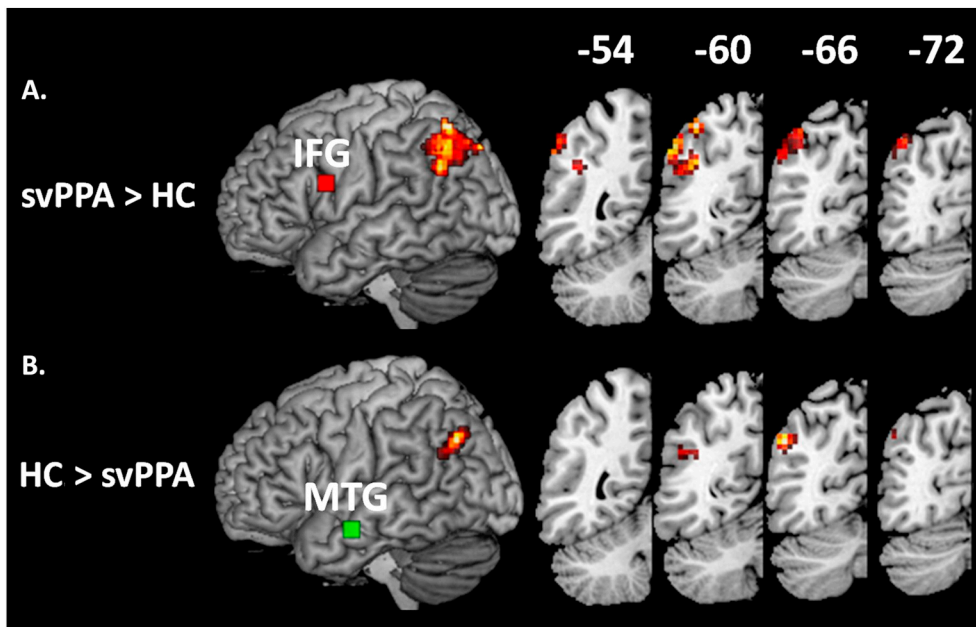


Fig. 4. Comparison of functional connectivity between svPPA patients and HC. SvPPA patients showed stronger connectivity with the opIFG seed in the upper part of the angular gyrus (panel A). Decreased connectivity with the aMTG seed was found in the lower part of the angular gyrus (panel B). Results were thresholded voxel-wise at $p < .01$ and corrected for family-wise error rate $p < .05$ at cluster level. Seeds are shown as red (opIFG seed) and green (aMTG seed) boxes on the surface rendering of the left hemisphere. Coronal IPL sections are shown for the left hemisphere.

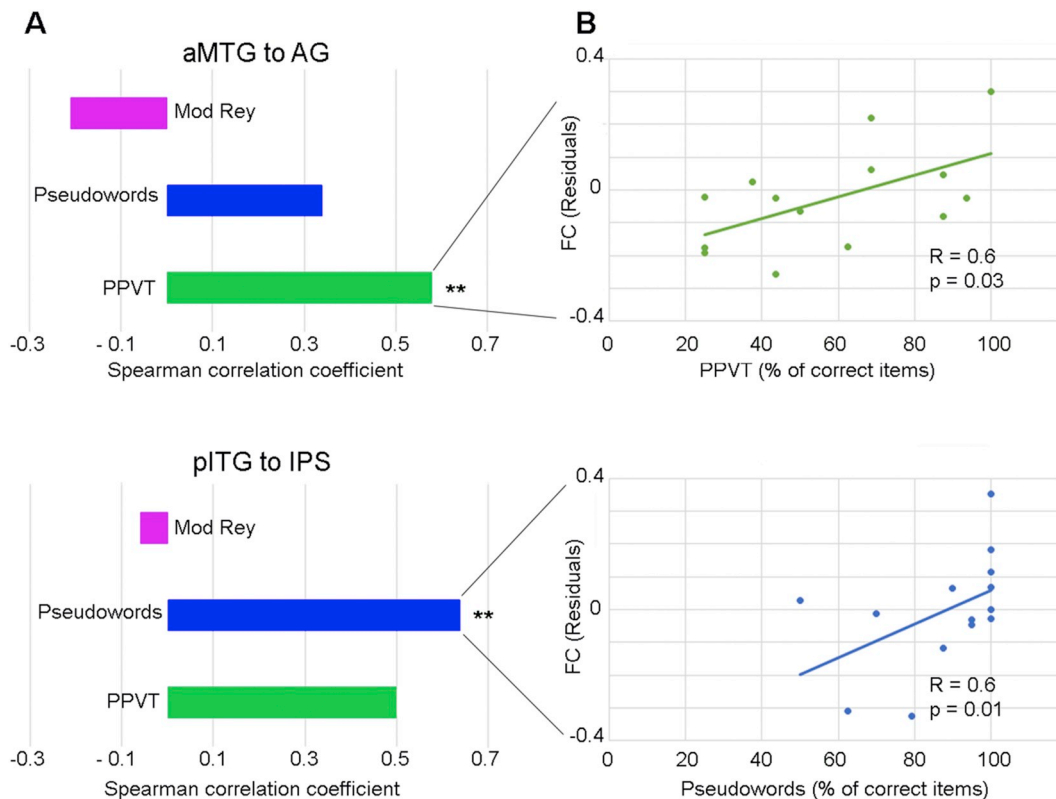


Fig. 5. Functional connectivity-behavioral correlations. Panel A highlights the dissociation of the language networks by showing that patients' performance only on the PPVT score significantly correlated with functional connectivity in the aMTG-to-AG network, while performance on Pseudoword reading correlated with pITG-to-IPS connectivity. The horizontal axis displays the Spearman correlation coefficients, and the vertical axis lists the names of the behavioral measures. Panel B shows the scatter plots of the significant correlations. The % of correct items in the behavioral scores (horizontal axes) were plotted against the residual of the functional connectivity scores after removing the effect of disease severity through the CDR score. The reported p -value is not corrected for multiple comparisons due to the small sample size.

4.2. Inferior frontal - to - supramarginal network and its role in fluency and phonology

The pars opercularis of the inferior frontal gyrus (opIFG) has been historically described as a key region supporting articulatory-

phonological processes, which are preserved in svPPA patients (Gorno-Tempini et al., 2004; Jefferies et al., 2005). Consistently, this network showed normal functional connectivity in individuals with svPPA. Using a left opIFG seed derived from a phonemic fluency task (Heim et al., 2008), we identified a network including fronto-parietal, medial

frontal, and basal ganglia regions, previously described as the speech production network (Mandelli et al., 2016). Within the parietal cortex, the cluster connected to opIFG was located in the SMG (BA 40) in controls, a region implicated in phonological assembly and phonological-motor integration (Rapcsak et al., 2009; Henry et al., 2012; Price, 2012; Henry et al., 2016). Anatomically, the opIFG is connected to the SMG through white matter fibers of the third portion of the superior longitudinal fasciculus (SLF III, Thiebaut de Schotten et al., 2012). Based on previous data and the known relative sparing of phonological and articulatory processes in svPPA, we hypothesized that this network would sustain fluency in our patients. Furthermore, the increase in connectivity between opIFG and the dorsal-posterior AG may reflect an enhancement of the dorsal articulatory-phonological system. It could be speculated that svPPA patients increasingly make use of IFG-mediated verbalization and phonological strategies during language tasks. Decreased connectivity of the ventral semantic network would result in increased overlap and connectivity between orthographical-phonological and motor speech systems, and a larger AG cortical hub. It is a clinical observation that when patients with mild svPPA cannot name an object, they often produce the name of the first letter of the word and even a few phonemes.

4.3. Anterior middle temporal - to - angular network and its role in semantics

The anterior middle temporal gyrus (aMTG), located posteriorly to svPPA patients' disease epicenter in the anterior temporal lobe, has been associated with semantic processing in this disorder and healthy subjects (Patterson et al., 2007a). In our study, the inferior AG (BA 39) emerged as the IPL sub-region most strongly linked to the aMTG. Anatomical studies in human and non-human primates show the existence of structural connections between these regions through fibers of the middle longitudinal fasciculus (Burks et al., 2017). This ventral temporo-parietal language network includes medial temporal and posterior cingulate regions, corresponding to portions of the default mode network (DMN); the activation of the DMN in task-free functional studies is well-established and has been associated with several cognitive processes (Greicius et al., 2003). This ventral system also has been consistently implicated in semantic processing in fMRI activation studies of healthy adults (see meta-analysis by Binder et al., 2009a), thus establishing its role in language comprehension and semantics (Gorno-Tempini et al., 1998; Binder et al., 2003; Mechelli et al., 2007; Seghier et al., 2010; Gesierich et al., 2012). However, the precise role of the AG hub is still controversial. Cognitive models suggest the AG's involvement in the retrieval or rapid combination of conceptual information, rather than formation and storage of conceptual representations (Jefferies and Lambon Ralph, 2006; Binder et al., 2009a). As the AG is not significantly atrophied in our and other groups of svPPA patients, the observed functional connectivity alteration in the AG is likely the result of a functional diaschisis with the degenerating aMTG. This finding highlights the network-wide and large-scale consequences of focal neurodegeneration (Guo et al., 2013; Collins et al., 2017). Therefore, the profound single word comprehension and semantic deficits in svPPA are likely due to, not only the atrophy of the aMTG, but also the dysfunction of the whole semantic network (Mummery et al., 1999). Consistently, the strength of connectivity in this ventral network correlated with deficits in the number of recognized words as measured by the Peabody Picture Vocabulary Test in svPPA, thus further supporting the role of this network in semantic processing.

4.4. Posterior inferior temporal - to - intraparietal network and its role in orthography and attention

The posterior ITG (pITG) is a key region that helps to link visual to linguistic processes in reading and naming studies. Atrophy in svPPA starts from the temporal lobe and progresses posteriorly, and thus, this

region usually is spared until the late stages of the disorder. The functional network derived from seeding in the pITG included areas in the bilateral ITG, left intraparietal sulcus (IPS), bilateral triangular IFG, and left precentral gyrus. Within the IPL, the region that connected to pITG primarily was centered in the IPS (BA 40), lying posteriorly to the SMG fluency hub and dorsally to the AG semantic hub (see Fig. 2). Anatomically, the IPS is connected to the pITG through temporo-parietal white matter fibers of the posterior segment of the SLF (Thiebaut de Schotten et al., 2012). The intrinsic connectivity pattern within the network in svPPA did not differ from that in healthy controls. This network involves regions commonly associated with both multimodal and orthographic language processes (Price and Friston, 1997; Cohen et al., 2004; Purcell et al., 2011; Fairhall and Caramazza, 2013). However, the specific role of this network in the multi-component reading process is still disputed. Individuals with svPPA typically show surface dyslexia, characterized by impaired exception word reading and relatively spared pseudo-word reading. A previous task-based fMRI study investigating the neural basis of reading in svPPA (Wilson et al., 2009) suggested that the IPS may be involved in sub-lexical reading. This area was activated in controls and svPPA patients when reading pseudo-words, which necessitates the application of sub-lexical orthography-to-phonology transformations. Additionally, the same region showed greater activation when svPPA patients made "over-regularization errors" on words with irregular spelling-to-sound correspondences (irregularly spelled words). This type of reading error has been described as an improper application of sub-lexical reading processes in the event of a failure to retrieve item-specific "semantic" information (Patterson and Hodges, 1992). In this study, connectivity metrics in this network correlated with patients' pseudoword reading scores, providing additional evidence for its role in sub-lexical reading. This posterior network is engaged preferentially when a visually-presented word is not recognized as a single unit, either because of its non-lexical status (i.e., pseudo-words) or because damage within the semantic hub impairs access to the associated word-specific pattern (as occurs with exception words in svPPA). The IPS may provide the attentional resources needed to scan the visually-represented letter string and segment it into plausible graphemes for subsequent conversion into the relevant phonemes. The finding that the IPS often is activated in spatial and feature-based attention tasks (Corbetta and Shulman, 2002; Vogel et al., 2012) favors this hypothesis.

4.5. Limitations

The current work relies on the comparison of functional connectivity profiles in healthy controls with a single variant of PPA. Further studies are needed to localize distinct and shared patterns of connectivity in the three variants of PPA (logopenic vs. non-fluent vs. semantic) and to fully characterize the differential involvement of the IPL in PPA. Moreover, further work is needed to investigate the behavioral relevance of the reorganization of the dorsal network observed in svPPA, and to probe its potential for therapeutic purposes. We acknowledge that in the correlation between pITG-to-IPS connectivity and the percentage of correctly read pseudo-words in svPPA, some patients were at ceiling in this behavioral measure. Future studies are needed to assess orthography-to-phonology conversion with more sensitive tasks that might be able to better capture the variance within the svPPA population.

5. Conclusion

Our study identifies three segregated task-free functional language networks anchored to seeds involved in spared and impaired (articulatory-phonological vs. semantic processes) language functions in svPPA. These networks are connected to discrete left IPL sub-regions, supporting this region's multidimensional role in language processing. Furthermore, our data provide evidence that changes in functional

connectivity of this region reflect not only the behavioral impairments observed in svPPA, but also possible neural adaptations. The unique neuroanatomical and linguistic profile observed in svPPA provides a compelling model for the functional interplay of these networks, reflecting up- or down- regulation in response to disease. Furthermore, identifying functional language networks in specific disease profiles characterized by loss and sparing of such functions, as seen in svPPA, represents a powerful model to study the neurobiology of language.

Acknowledgments

The authors thank the patients and their families for the time and effort they dedicated to the research. The authors declare no competing financial interests.

Funding

The study was supported by grants from the National Institutes of Health (NINDS R01NS050915, NIDCD K24DC015544, NIDCD R03DC013403, NIDCD F32DC009145, NIDCD R01DC013270, NIDCD R01DC016291, NIDCD R01DC016345, NIA U01AG052943, NIA P50AG023501, NIA P01AG019724, NIA R01AG038791, NINDS U54NS092089); Alzheimer's Disease Research Center of California (03-75271 DHS/ADP/ARCC); Larry L. Hillblom Foundation; John Douglas French Alzheimer's Foundation; Koret Family Foundation; Consortium for Frontotemporal Dementia Research; and McBean Family Foundation.

Appendix A. Supplementary data

Supplementary data to this article can be found online at <https://doi.org/10.1016/j.nicl.2019.101797>.

References

- Achal, S., Hoeff, F., Bray, S., 2016. Individual differences in adult Reading are associated with left temporo-parietal to dorsal striatal functional connectivity. *Cereb. Cortex* 26 (10), 4069–4081.
- Agosta, F., Galantucci, S., Valsasina, P., Canu, E., Meani, A., Marcone, A., et al., 2014. Disrupted brain connectome in semantic variant of primary progressive aphasia. *Neurobiol. Aging* 35 (11), 2646–2655.
- Ashburner, J., Friston, K.J., 2005. Unified segmentation. *Neuroimage* 26 (3), 839–851.
- Baldo, J.V., Arevalo, A., Patterson, J.P., Dronkers, N.F., 2013. Grey and white matter correlates of picture naming: evidence from a voxel-based lesion analysis of the Boston Naming Test. *Cortex* 49 (3), 658–667.
- Beeson, P.M.R., 2010. K. Arizona Battery for Reading and Spelling (ABRS). (cited; Available from:).
- Binder, J.R., McKiernan, K.A., Parsons, M.E., Westbury, C.F., Possing, E.T., Kaufman, J.N., et al., 2003. Neural correlates of lexical access during visual word recognition. *J. Cogn. Neurosci.* 15 (3), 372–393.
- Binder, J.R., Desai, R.H., Graves, W.W., Conant, L.L., 2009a. Where is the semantic system? A critical review and meta-analysis of 120 functional neuroimaging studies. *Cereb. Cortex* 19 (12), 2767–2796.
- Binder, J.R., Desai, R.H., Graves, W.W., Conant, L.L., 2009b. Where is the semantic system? A critical review and meta-analysis of 120 functional neuroimaging studies. *Cereb. Cortex* 19 (12), 2767–2796.
- Binney, R.J., Henry, M.L., Babiak, M., Pressman, P.S., Santos-Santos, M.A., Narvid, J., et al., 2016. Reading words and other people: a comparison of exception word, familiar face and affect processing in the left and right temporal variants of primary progressive aphasia. *Cortex* 82, 147–163.
- Bonilha, L., Moser, D., Rorden, C., Baylis, G.C., Fridriksson, J., 2006. Speech apraxia without oral apraxia: can normal brain function explain the physiopathology? *Neuroreport* 17 (10), 1027–1031.
- Brunswick, N., McCrory, E., Price, C.J., Frith, C.D., Frith, U., 1999. Explicit and implicit processing of words and pseudowords by adult developmental dyslexics: a search for Wernicke's Wortschatz? *Brain* 122 (Pt 10), 1901–1917.
- Burks, J.D., Boettcher, L.B., Conner, A.K., Glenn, C.A., Bonney, P.A., Baker, C.M., et al., 2017. White matter connections of the inferior parietal lobule: a study of surgical anatomy. *Brain Behav.* 7 (4), e00640.
- Casanova, R., Srikanth, R., Baer, A., Laurienti, P.J., Burdette, J.H., Hayasaka, S., et al., 2007. Biological parametric mapping: a statistical toolbox for multimodality brain image analysis. *Neuroimage* 34 (1), 137–143.
- Caspers, S., Geyer, S., Schleicher, A., Mohlberg, H., Amunts, K., Zilles, K., 2006. The human inferior parietal cortex: cytoarchitectonic parcellation and interindividual variability. *Neuroimage* 33 (2), 430–448.
- Cohen, L., Jobert, A., Le Bihan, D., Dehaene, S., 2004. Distinct unimodal and multimodal regions for word processing in the left temporal cortex. *Neuroimage* 23 (4), 1256–1270.
- Collins, J.A., Montal, V., Hochberg, D., Quimby, M., Mandelli, M.L., Makris, N., et al., 2017. Focal temporal pole atrophy and network degeneration in semantic variant primary progressive aphasia. *Brain* 140 (2), 457–471.
- Corbetta, M., Shulman, G.L., 2002. Control of goal-directed and stimulus-driven attention in the brain. *Nat. Rev. Neurosci.* 3 (3), 201–215.
- Fairhall, S.L., Caramazza, A., 2013. Brain regions that represent amodal conceptual knowledge. *J. Neurosci.* 33 (25), 10552–10558.
- Foundas, A.L.D., Vasterling, J.J., 1998. Anomia: case studies with lesion localization. *Neurocase* 4, 35–43.
- Garcea, F.E., Mahon, B.Z., 2014. Parcellation of left parietal tool representations by functional connectivity. *Neuropsychologia* 60, 131–143.
- Gerstmann, J., 1957. Some notes on the Gerstmann syndrome. *Neurology* 7, 866–869.
- Gesierich, B., Jovicich, J., Riello, M., Adriani, M., Monti, A., Brentari, V., et al., 2012. Distinct neural substrates for semantic knowledge and naming in the temporoparietal network. *Cereb. Cortex* 22 (10), 2217–2226.
- Gorno-Tempini, M.L., Price, C.J., Josephs, O., Vandenberghe, R., Cappa, S.F., Kapur, N., et al., 1998. The neural systems sustaining face and proper-name processing. *Brain* 121 (Pt 11), 2103–2118.
- Gorno-Tempini, M.L., Cipolotti, L., Price, C.J., 2000. Category differences in brain activation studies: where do they come from? *Proc. Biol. Sci.* 267 (1449), 1253–1258.
- Gorno-Tempini, M.L., Dronkers, N.F., Rankin, K.P., Ogar, J.M., Phengrasamy, L., Rosen, H.J., et al., 2004. Cognition and anatomy in three variants of primary progressive aphasia. *Ann. Neurol.* 55 (3), 335–346.
- Gorno-Tempini, M.L., Brambati, S.M., Ginex, V., Ogar, J., Dronkers, N.F., Marcone, A., et al., 2008. The logopenic/phonological variant of primary progressive aphasia. *Neurology* 71 (16), 1227–1234.
- Gorno-Tempini, M.L., Hillis, A.E., Weintraub, S., Kertesz, A., Mendez, M., Cappa, S.F., et al., 2011. Classification of primary progressive aphasia and its variants. *Neurology* 76 (11), 1006–1014.
- Greicius, Michael D., Krasnow, Ben, Reiss, Allan L., Menon, Vinod, January 7, 2003. Functional connectivity in the resting brain: A network analysis of the default mode hypothesis. *PNAS* 100 (1), 253–258. <https://doi.org/10.1073/pnas.0135058100>.
- Grossman, M., 2012. The non-fluent/agrammatic variant of primary progressive aphasia. *Lancet Neurol.* 11 (6), 545–555.
- Guo, C.C., Gorno-Tempini, M.L., Gesierich, B., Henry, M., Trujillo, A., Shany-Ur, T., et al., 2013. Anterior temporal lobe degeneration produces widespread network-driven dysfunction. *Brain* 136, 2979–2991 Pt 10.
- Heim, S., Eickhoff, S.B., Amunts, K., 2008. Specialisation in Broca's region for semantic, phonological, and syntactic fluency? *Neuroimage* 40 (3), 1362–1368.
- Henry, M.L., Beeson, P.M., Alexander, G.E., Rapcsak, S.Z., 2012. Written language impairments in primary progressive aphasia: a reflection of damage to central semantic and phonological processes. *J. Cogn. Neurosci.* 24 (2), 261–275.
- Henry, M.L., Wilson, S.M., Babiak, M.C., Mandelli, M.L., Beeson, P.M., Miller, Z.A., et al., 2016. Phonological processing in primary progressive aphasia. *J. Cogn. Neurosci.* 28 (2), 210–222.
- Hillis, A.E., Work, M., Barker, P.B., Jacobs, M.A., Breese, E.L., Maurer, K., 2004. Re-examining the brain regions crucial for orchestrating speech articulation. *Brain* 127, 1479–1487 Pt 7.
- Hodges, J.R., Patterson, K., Oxbury, S., Funnell, E., 1992. Semantic dementia. Progressive fluent aphasia with temporal lobe atrophy. *Brain* 115, 1783–1806 Pt 6.
- Humphreys, G.F., Lambon Ralph, M.A., 2015. Fusion and fission of cognitive functions in the human parietal cortex. *Cereb. Cortex* 25 (10), 3547–3560.
- Jackson, R.L., Hoffman, P., Pobric, G., Lambon Ralph, M.A., 2016. The semantic network at Work and rest: differential connectivity of anterior temporal lobe subregions. *J. Neurosci.* 36 (5), 1490–1501.
- Jefferies, E., Lambon Ralph, M.A., 2006. Semantic impairment in stroke aphasia versus semantic dementia: a case-series comparison. *Brain* 129, 2132–2147 Pt 8.
- Jefferies, E., Jones, R.W., Bateman, D., Ralph, M.A., 2005. A semantic contribution to nonword recall? Evidence for intact phonological processes in semantic dementia. *Cogn. Neuropsychol.* 22 (2), 183–212.
- Jung, J., Visser, M., Binney, R.J., Lambon Ralph, M.A., 2018. Establishing the cognitive signature of human brain networks derived from structural and functional connectivity. *Brain Struct. Funct.* 223 (9), 4023–4038.
- Kertesz, A., 1982. Western Aphasia Battery Test Manual. The University of Virginia: Grune & Stratton.
- Kramer, J.H., Jurik, J., Sha, S.J., Rankin, K.P., Rosen, H.J., Johnson, J.K., et al., 2003. Distinctive neuropsychological patterns in frontotemporal dementia, semantic dementia, and Alzheimer disease. *Cogn. Behav. Neurol.* 16 (4), 211–218.
- MacSweeney, M., Brammer, M.J., Waters, D., Goswami, U., 2009. Enhanced activation of the left inferior frontal gyrus in deaf and dyslexic adults during rhyming. *Brain* 132, 1928–1940 Pt 7.
- Maldjian, J.A., Laurienti, P.J., Kraft, R.A., Burdette, J.H., 2003. An automated method for neuroanatomic and cytoarchitectonic atlas-based interrogation of fMRI data sets. *Neuroimage* 19 (3), 1233–1239.
- Mandelli, M.L., Vilaplana, E., Brown, J.A., Hubbard, H.I., Binney, R.J., Attygalle, S., et al., 2016. Healthy brain connectivity predicts atrophy progression in non-fluent variant of primary progressive aphasia. *Brain* 139, 2778–2791 Pt 10.
- Mechelli, A., Josephs, O., Lambon Ralph, M.A., McClelland, J.L., Price, C.J., 2007. Dissociating stimulus-driven semantic and phonological effect during reading and naming. *Hum. Brain Mapp.* 28 (3), 205–217.
- Mesulam, M.M., 2001. Primary progressive aphasia. *Ann. Neurol.* 49 (4), 425–432.
- Mion, M., Patterson, K., Acosta-Cabrero, J., Pengas, G., Izquierdo-Garcia, D., Hong, Y.T., et al., 2010. What the left and right anterior fusiform gyri tell us about semantic

- memory. *Brain* 133 (11), 3256–3268.
- Mummary, C.J., Patterson, K., Wise, R.J., Vandenberghe, R., Price, C.J., Hodges, J.R., 1999. Disrupted temporal lobe connections in semantic dementia. *Brain* 122 (Pt 1), 61–73.
- Nelson, S.M., Cohen, A.L., Power, J.D., Wig, G.S., Miezin, F.M., Wheeler, M.E., et al., 2010. A parcellation scheme for human left lateral parietal cortex. *Neuron* 67 (1), 156–170.
- Noppeney, U., Patterson, K., Tyler, L.K., Moss, H., Stamatakis, E.A., Bright, P., et al., 2007. Temporal lobe lesions and semantic impairment: a comparison of herpes simplex virus encephalitis and semantic dementia. *Brain* 130 (Pt 4), 1138–1147.
- Patterson, K., Hodges, J.R., 1992. Deterioration of word meaning: implications for reading. *Neuropsychologia* 30 (12), 1025–1040.
- Patterson, K., Nestor, P.J., Rogers, T.T., 2007a. Where do you know what you know? The representation of semantic knowledge in the human brain. *Nat. Rev. Neurosci.* 8 (12), 976–987.
- Patterson, K., Nestor, P.J., Rogers, T.T., 2007b. Where do you know what you know? The representation of semantic knowledge in the human brain. *Nat. Rev. Neurosci.* 8 (12), 976–987.
- Pievani, M., Filippini, N., van den Heuvel, M.P., Cappa, S.F., Frisoni, G.B., 2014. Brain connectivity in neurodegenerative diseases—from phenotype to proteinopathy. *Nat. Rev. Neurol.* 10 (11), 620–633.
- Podzebenko, K., Egan, G.F., Watson, J.D., 2005. Real and imaginary rotary motion processing: functional parcellation of the human parietal lobe revealed by fMRI. *J. Cogn. Neurosci.* 17 (1), 24–36.
- Price, C.J., 2000. The anatomy of language: contributions from functional neuroimaging. *J. Anat.* 197 (Pt 3), 335–359.
- Price, C.J., 2012. A review and synthesis of the first 20 years of PET and fMRI studies of heard speech, spoken language and reading. *Neuroimage* 62 (2), 816–847.
- Price, C.J., Friston, K.J., 1997. The temporal dynamics of reading: a PET study. *Proc. Biol. Sci.* 264 (1389), 1785–1791.
- Price, C.J., Crinion, J., Friston, K.J., 2006. Design and analysis of fMRI studies with neurologically impaired patients. *J. Magn. Reson. Imaging* 23 (6), 816–826.
- Purcell, J.J., Turkeltaub, P.E., Eden, G.F., Rapp, B., 2011. Examining the central and peripheral processes of written word production through meta-analysis. *Front. Psychol.* 2, 239.
- Raichle, M.E., 2006. Neuroscience. The brain's dark energy. *Science* 314 (5803), 1249–1250.
- Rapcsak, S.Z., Beeson, P.M., Henry, M.L., Leyden, A., Kim, E., Rising, K., et al., 2009. Phonological dyslexia and dysgraphia: cognitive mechanisms and neural substrates. *Cortex* 45 (5), 575–591.
- Ruschel, M., Knosche, T.R., Friederici, A.D., Turner, R., Geyer, S., Anwander, A., 2014. Connectivity architecture and subdivision of the human inferior parietal cortex revealed by diffusion MRI. *Cereb. Cortex* 24 (9), 2436–2448.
- Schwartz, M.F., Kimberg, D.Y., Walker, G.M., Faseyitan, O., Brecher, A., Dell, G.S., et al., 2009. Anterior temporal involvement in semantic word retrieval: voxel-based lesion-symptom mapping evidence from aphasia. *Brain* 132, 3411–3427 Pt 12.
- Seeley, W.W., Crawford, R.K., Zhou, J., Miller, B.L., Greicius, M.D., 2009. Neurodegenerative diseases target large-scale human brain networks. *Neuron* 62 (1), 42–52.
- Seghier, M.L., Fagan, E., Price, C.J., 2010. Functional subdivisions in the left angular gyrus where the semantic system meets and diverges from the default network. *J. Neurosci.* 30 (50), 16809–16817.
- Simmons, W.K., Reddish, M., Bellgowan, P.S., Martin, A., 2010. The selectivity and functional connectivity of the anterior temporal lobes. *Cereb. Cortex* 20 (4), 813–825.
- Sonty, S.P., Mesulam, M.M., Thompson, C.K., Johnson, N.A., Weintraub, S., Parrish, T.B., et al., 2003. Primary progressive aphasia: PPA and the language network. *Ann. Neurol.* 53 (1), 35–49.
- Stevens, W.D., Kravitz, D.J., Peng, C.S., Tessler, M.H., Martin, A., 2017. Privileged functional connectivity between the visual word form area and the language system. *J. Neurosci.* 37 (21), 5288–5297.
- Tahmasian, M., Shao, J., Meng, C., Grimmer, T., Diehl-Schmid, J., Yousefi, B.H., et al., 2016. Based on the network degeneration hypothesis: separating individual patients with different neurodegenerative syndromes in a preliminary hybrid PET/MR study. *J. Nucl. Med.* 57 (3), 410–415.
- Thiebaut de Schotten, M., Dell'Acqua, F., Valabregue, R., Catani, M., 2012. Monkey to human comparative anatomy of the frontal lobe association tracts. *Cortex* 48 (1), 82–96.
- Tzourio-Mazoyer, N., Landeau, B., Papathanassiou, D., Crivello, F., Etard, O., Delcroix, N., et al., 2002. Automated anatomical labeling of activations in SPM using a macroscopic anatomical parcellation of the MNI MRI single-subject brain. *Neuroimage* 15 (1), 273–289.
- Vandenberghe, R., Price, C., Wise, R., Josephs, O., Frackowiak, R.S., 1996. Functional anatomy of a common semantic system for words and pictures. *Nature* 383 (6597), 254–256.
- Vogel, A.C., Miezin, F.M., Petersen, S.E., Schlaggar, B.L., 2012. The putative visual word form area is functionally connected to the dorsal attention network. *Cereb. Cortex* 22 (3), 537–549.
- Wang, J., Zhang, J., Rong, M., Wei, X., Zheng, D., Fox, P.T., et al., 2016. Functional topography of the right inferior parietal lobule structured by anatomical connectivity profiles. *Hum. Brain Mapp.* 37 (12), 4316–4332.
- Wang, J., Xie, S., Guo, X., Becker, B., Fox, P.T., Eickhoff, S.B., et al., 2017. Correspondent functional topography of the human left inferior parietal lobule at rest and under task revealed using resting-state fMRI and coactivation based parcellation. *Hum. Brain Mapp.* 38 (3), 1659–1675.
- Weissenbacher, A., Kasess, C., Gerstl, F., Lanzenberger, R., Moser, E., Windischberger, C., 2009. Correlations and anticorrelations in resting-state functional connectivity MRI: a quantitative comparison of preprocessing strategies. *Neuroimage* 47 (4), 1408–1416.
- Wilson, S.M., Brambati, S.M., Henry, R.G., Handwerker, D.A., Agosta, F., Miller, B.L., et al., 2009. The neural basis of surface dyslexia in semantic dementia. *Brain* 132, 71–86 Pt 1.
- Wilson, S.M., Henry, M.L., Besbris, M., Ogar, J.M., Dronkers, N.F., Jarrold, W., et al., 2010. Connected speech production in three variants of primary progressive aphasia. *Brain* 133, 2069–2088 Pt 7.
- Yarkoni, T., Poldrack, R.A., Nichols, T.E., Van Essen, D.C., Wager, T.D., 2011. Large-scale automated synthesis of human functional neuroimaging data. *Nat. Methods* 8 (8), 665–670.